Development Experimental Investigations of Truss Bridge Model for Vibration-Based Structural Health Monitoring

Sukamta, Angga Alfiannur, Susilo Adi Widyanto, and Han Ay Lie

Abstract In recent years the need for Structural Health Monitoring (SHM) has become increasingly important. Given current technological developments, a visual inspection can no longer be a reference due to inaccurate accuracy levels. In this case, there is a need for an early warning in detecting fast and accurate damage compared to visual inspection. This study proposes a vibration-based structural health monitoring analytical framework by introducing a modal analysis approach based on the bridges structural response. The test begins with making a small-scale model of a steel frame type bridge using the similarity model theory to project a prototype bridge. In this research, a damage simulation is given to the model to project damage to the structure. Static and dynamic tests are carrying to obtain the response characteristics of the structure. The assessment has delayed consequences exhibit that the variety of the supported discharge shows that contrasts look like the bend of the predominant recurrence that influences the FFT bend. Output values in natural frequency, mode shapes, and capital damping ratios were adopted as damage indicators. As a comparison, we are testing the model using FE simulation with a tolerance level of 10%. This research is using to build an SHM database system of the existing bridge structure model.

Keywords Vibration-based health monitoring · Steel bridges · Modal analysis · Small scale model

Sukamta (✉) · H. A. Lie
Department of Civil Engineering, Diponegoro University, Semarang, Indonesia

H. A. Lie
e-mail: hanaylie@live.undip.ac.id

A. Alfiannur
Master Program in Civil Engineering, Diponegoro University, Semarang, Indonesia

S. A. Widyanto
Department of Mechanical Engineering, Diponegoro University, Semarang, Indonesia

S. Belayutham et al. (eds.), *Proceedings of the 5th International Conference on Sustainable Civil Engineering Structures and Construction Materials*, Lecture Notes in Civil Engineering 215, https://doi.org/10.1007/978-981-16-7924-7_9

1 Introduction

Structural health monitoring (SHM) in recent years has become very important. Along with current technological developments and the many requests for monitoring, structural health monitoring such as bridges caused by deteriorating structural conditions due to age and damage due to natural disasters. Vibration-based SHM has become one of the efforts that have received attention in recent years to detect a malfunction [1, 2].

Damage detection methods are currently the most widely used visual observations made by bridge experts. This method is inaccurate and requires a long time, mainly if the observed bridge is locating in a difficult-to-reach location with large dimensions. Visual inspection is very dependent on the examiner's condition and, in certain conditions, can endanger the examiner itself. Also, structural damage is observing on exposed surfaces, and it is difficult to observe the damage that is hiding in nature, so it is not easily observed directly [3].

The vibration-based SHM technique requires identifying the dynamic characteristics of the bridge through field vibration measurements. Taking advantage of modern technology capabilities, such as vibration data, is obtained remotely, which allows for real-time monitoring of bridge conditions [4]. Damage that occurs in the structure causes changes in the stiffness and damping properties of the global structure so that it affects dynamic characteristics such as mode shape, natural frequency, and damping ratio [3, 5, 6]. The method of detecting damage using the vector shape mode as a feature generally analyzes the difference between the modal vectors measured before and after the damage. The mode shape vector is a spatially distributed number, and the data is using to detect damage [7].

The proposed vibration-based SHM approach can promise the ability to detect damage at the local level when problems related to sensitivity, low frequency, and mode shape result from local damage. Damage detection by changing the stiffness parameter using an updated finite element model utilizes data from a large number of sensors [1]. Time–frequency analysis is significant for damage detection because it is more sensitive to damage when the dynamics change from various conditions [8]. Another thing to note is that the optimal experimental design method refers to an algorithm to optimize the structures location and many sensors. The measurement data obtained contains the most important information for structural identification purposes.

In this study, the proposed framework uses a vibration mode in the form of deterministic vibrations. The amount of dynamic excitation (force or motion) acting on the system can be adjusting according to the need. The raw data from these vibrations are processed using Fast Fourier Transform to obtain the time domain signals vibration spectrum and determine the damaged structures natural frequency. The next process is to analyze the damping ratio to determine the degree of change in the structures attenuation characteristics when there is damage.

In these studies, structural testing in the Laboratory often requires a scaled model for testing. Bridges generally have large dimensions and heavy loads. Therefore, they

require a scale to suit laboratory facilities, costs, and testing schedules. However, the model scale is not an easy procedure, requiring the fulfilment of special requirements stemming from the same analysis. A steel truss bridge is using with the case study of Sendang Mulyo Bridge, Semarang Indonesia.

This research is the initial stage of SHM testing based on vibration, where this study models the actual bridge (Prototype) on a small scale. It aims to gain theoretical insight into global damage detection causes, leading to practical and useful vibration-based SHM.

2 Vibrate Mode

2.1 Fast Fourier Transform (FFT)

An appropriate numerical way for computers to determine the frequency and time domains response is the fast Fourier transform (FFT) [9]. With a single degree of freedom due to a force, the systems response is given by Eq. (1), which is expressed as an exponential function.

$$A(j) = \sum_{n=0}^{N-1} A^{(0)}(n) W_N^{jn} \tag{1}$$

where

$$W_N = e^{2\pi i/N} \tag{2}$$

The evaluation of addition will be more effective if the number of time increments of N, the divisor in period T, is a square number.

$$N = M^2 \tag{3}$$

M is an integer; in this case, the integers j and n were expressing in the "binary" form. As an illustration, consider a simple condition in which the load period is divide into eight increment intervals: N = 8, M = 3. In this situation, the indices have a binary form,

$$\begin{aligned} j &= j_0 + 2j_1 + 4j_2 \\ n &= n_0 + 2n_1 + 4n_2 \end{aligned} \tag{4}$$

and Eq. (3) can be written as

$$A(j) = \sum_{n_2=0}^{1} \sum_{n_1=0}^{1} \sum_{n0=0}^{1} A^{(0)}(n) W_8^{(j_0+2j_1+4j_2+)(n_0+2n_1+4n_2)}$$
$$W_8^{jn} = W_8^{8(j_1n_2+2j_2n_2+j_2n_1)} W_8^{4n_2j_0} W_8^{2n_1(2j_1+j_0)} W_8^{n_0(4j_2+2j_1+j_0)} \quad (5)$$

It might be seeing that the principal factor on the privilege is worth one in light of Eq. (2).

$$W_8^{8I} = e^{2\pi i(8/8)I} = \cos 2\pi I + i \sin 2\pi I = 1 \quad (6)$$

where $I = j_1n_2 + 2j_2n_2 + j_2n_1$ is an integer. Therefore, only three factors remain that need to be considered in the summation.

These summations can be carried out accurately and persistently by introducing a new notation that indicates the addition process is the correct step. The first step that is showing is.

$$A^{(1)}(j_0, n_1, n_0) = \sum_{n=1}^{1} A^{(0)}(n_2, n_1, n_0) W_8^{4n_2j_0} \quad (7)$$

where $A^{(0)}(n_2, n_1, n_0) = A^{(0)}(n)$ in Eq. (3) in the same way, do it for M = 2 and M = 3.

2.2 *Half Power Bandwidth Method for Damping Analysis*

The bandwidth method is the difference between two frequencies concerning the same amplitude response related to attenuation in a system [9]. The curved shape of the amplitude of a frequency is obtained experimentally for an ordinary damped structure. In the evaluation of damping, it is appropriate to measure the bandwidth at $1/\sqrt{2}$ times the amplitude given by Eq. (8) that is,

$$\frac{y_{st}}{\sqrt{\left(1-r^2\right)^2 + (2r\xi)^2}} = \frac{1}{\sqrt{2}} \frac{y_{st}}{2r\xi} \quad (8)$$

It is solving by squaring the two sides to give the frequency ratio.

$$r^2 = 1 - 2\xi\sqrt{1+\xi^2} \quad (9)$$

Finally, the damping ratio is giving almost half the difference between the frequency ratios of the two "half-powers," that is,

$$\zeta = \frac{\omega b - \omega a}{2\omega n} \text{ a tau } \zeta = \frac{fb - fa}{2fn} \tag{10}$$

3 Experimental Program

3.1 Small Scale Bridge Bride for Model Fabrication

In this research, the case study (prototype) is the Sendang Mulyo Bridge, a steel-frame bridge built-in 1996 over a river for road traffic. Overall, the sections on the Sendang Mulyo Bridge consist of 3 parts, namely the side/horizontal part, the upper part (wind tie), and the lower part (deck), with a total length of the bridge of 53 m, a width of 9.3 m and a bridge height of 5 m. The type of steel profile used on the primary side is IWF 300.300.10.25, the upper side uses IWF 300.300.10.15, the upper (wind bond) uses 200.200.8.12, and the lower part (deck) uses IWF 300.300.10.15. The bridge consists of a composite deck of steel beams and reinforced concrete slabs with a thickness of 35 cm.

The prototype bridge was made into a small-scale bridge based on Pi Theorem Buckingham theory to get the bridges same characteristics [7]. The bridge model structure uses a 1:23 scale geometry determined based on the availability of types and profiles available in the market. In this study, the bridge model structure uses hollow steel 15 × 15 mm with 1.2 mm thickness. The connection between modules uses a steel plate with a 2 mm thickness using a steel bolt connection sized M4. To represent the road plane, the bridge model uses a 2 mm thick plate. In the deck, a welding connection system is using. Figure 1 shows the results of the small-scale model of the bridge.

3.2 Vibration Measurement Instruments

In this study, to simulate the load of vehicles passing the bridge, a dynamic loading system is used in the form of a rotating unbalance mass. The working system of an unbalance or excitation mass generator is a force generated from centrifugal force. The characteristics of the vibrations caused by excitation are deterministic (periodic) vibrations. The excitation forces magnitude was vibrated equal to the structure's natural frequency using the bump test method on a small-scale bridge model. Table 1 shows the specifications of the unbalance mass.

This study, accelerometer sensor uses a 3 Axis-ADXL 355 type sensor with a sensitivity of each axis (X, Y, Z) max is 330 mV / g. Each vibration sensor unit uses an accelerometer with a power system, signal conditional, and transmitter system. Two

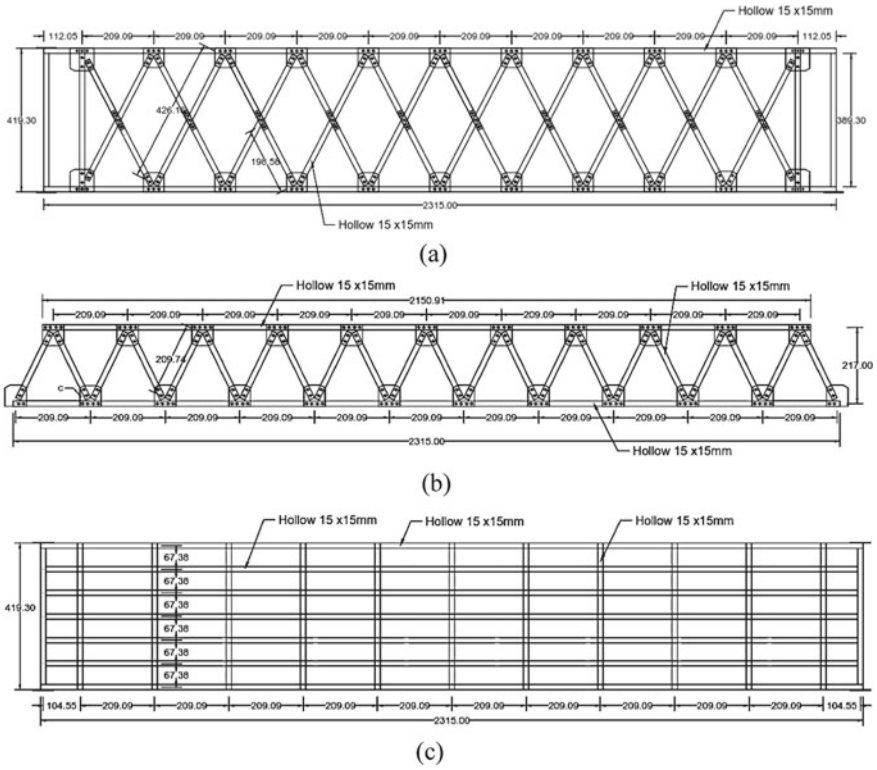

Fig. 1 Scale model 1:23: **a** Top view; **b** Side view; **c** Bottom view

Table 1 Specifications of unbalance mass

Specification	Unit	Value
Unbalance mass	g	5
Force	N	1064
Frequency	Hz	39–40
Turning radius	mm	10

accelerometer sensors are placed on the side diagonal bars to record the vibrations of the structure.

3.3 Simulation of Damage and Test Preparation

Table 2 presents the various damage simulations performed. The damage was simulating with two methods: the first method by performing the bar release (V-B) on the diagonal bar element. The second method is to reduce the bar inertia by 50% on the

Table 2 Damage simulation variations

Variation	Damage simulation position				Information
	V1	V2	V3	V4	
N	–	–	–	–	Normal
V-B	√	√	√	√	Bar release
V-50%	√	√	√	√	Bar inertia reduction 50%

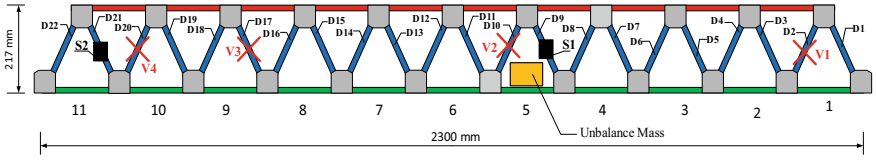

Fig. 2 Sensor position, excitation, and damage position

diagonal bar element (V-50%). The damage representation simulates a real-world vibration monitoring problem, where the location and size of the damage are both unknown. This study uses a variation of the V-B damage due to the software limited ability to compare experimental results with FE simulation. Damage simulation is useful for seeing the magnitude of changes in the vibration characteristics of the bridge model (Fig. 2).

Figure 3 presents the layout of the test settings and damage simulation. The sensor installation location considers the sensitivity of the sensor in detecting damage by paying attention to the position of the damaged bar and the mass load (excitation) on the bridge model. The dynamic excitation placement on the bridge deck is located on element 5. Sensor 1 (S1) is located close to the excitation/vibration source, namely on the diagonal rod element D9, and sensor 2 (S2) is located on the diagonal bar element D21 from the source of the vibration.

The initial process of testing the vibration mode is to perform a short test under Normal (N) conditions. In this condition, the bridge is new or not damaged. After getting the natural frequency from condition N, the next step is to test the damage simulation in the bar release condition (V-B). The simulation of V-B damage starts from position V1 to position V4. The position of V1 is on the diagonal bar D2, and then the rod will be released for vibration recording to be carried out. After obtaining the vibration mode data in condition V1, the diagonal bar D2 is again installed in its position and continued with V2, which is on the D10 bar for vibration mode recording. This process is valid until the position of V4 on the diagonal bar of D20. In the V-50% damage simulation, one new diagonal bar has reduced the inertia in the cross-section, replacing the diagonal bar installed at each damage simulation position. The stages of recording the vibration mode data in the V-50% condition is the same as during the V-B conditions.

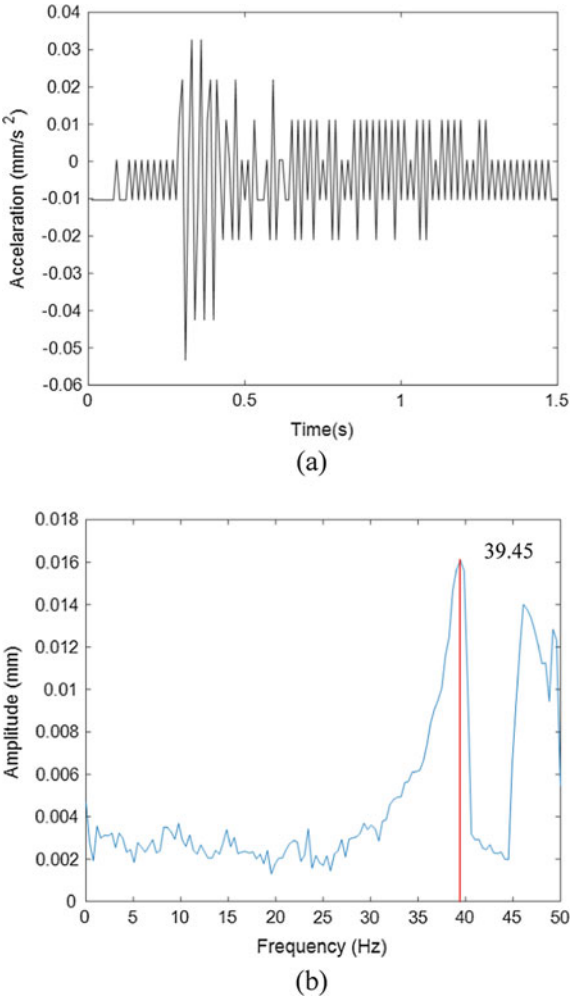

Fig. 3 The results of the bump test on the bridge model: **a** Time-domain; **b** Frequency-domain

3.4 Data Processing

During the recording process, the data obtained is the time domain structure-acceleration (time-domain). The domain response is then transformed into a frequency-amplitude domain using the Fast Fourier Transform (FFT) method. The FFT transformation will see that the natural frequency of the structure is indicated by the frequency of the peak value of the frequency—amplitude (frequency domain) curve.

Data is usually seen on the frequency—amplitude curve on the response to vibration and structural disturbances (noise). Identification is needed to ensure that the

Table 3 Simulation model results for frequency

Variation	Frequency (Hz)
Normal	41.908
V1	42.191
V2	41.962
V3	40.529
V4	40.232

peak amplitude responds to structural vibrations, which will later obtain the structures natural frequency. The half-power bandwidth method is used to determine the vibration damping ratio. The final step is to simulate the bridge model using FE to get the theoretical natural frequency, which helps validate the bridge model experimental test results against the structures natural frequency.

4 Result and Discussion

4.1 Identification Natural Frequency FE Model

Table 3 shows the results of testing natural frequencies on the FEA and bar release variations. Modal analysis in the FEA model produces a natural frequency, wherein this study, the first mode form used for comparison with experimental model testing. In this mode, the type of vibration obtained is transverse bending.

The results of global vibration identification produce different frequency values. In the N condition, the natural frequency is 41.908 Hz. Natural frequency tends to decrease after damage simulation is carried out in a row from conditions V1, V2, V3, and V4 of 42.191, 41.962, 41.529, and 41.232 Hz. Changes in frequency occur due to deformation changes, which result in stress concentrations in the bridge model structure.

4.2 Natural Frequency of Bridge Model Structures

The natural frequency value of the bridge model is obtained using the bump test method. A bump test using a 12 N object dropped 10 cm into the bridge model deck center. The test results can be seen in Fig. 3.

From the results of the graphical FFT analysis shown in Fig. 3b, it can be seen that the natural vibration frequency of the structure is at a frequency of 39 to 40 Hz with a peak of 39.45 Hz. The natural frequency obtained is used to reference the vibrations magnitude, given by the excitation/signal generator.

4.3 V-B Vibration Mode Measurement

Before measuring the vibration on the bridge model structures condition, it is necessary to measure the frequency generated by excitation. Unbalance mass setting at a rotational speed of ± 2340 RPM or around 39–40 Hz. It was recorded in vibration mode for 10 s with a sampling rate of 100 samples/second. Especially for the V–B damage simulation, data collection is carried out on N, V1, V2, V3, and V4 for S1 and S2. The natural frequency analyzed by Fast Fourier Transform (FFT) between S1 and S2 produces a similar frequency. The difference occurs in the amplitude value of the vibration.

. At the resulting peak amplitude, not all of them can be identified as the natural frequency of the structure because there is noise such as the new peak amplitude, as shown in Fig. 4. To be able to identify which is a natural frequency or noise, repeated checking is done, which is the highest peak amplitude appears on every measurement or not. If the highest peak occurs at each measurement, the amplitude-frequency is the natural frequency of the structure.

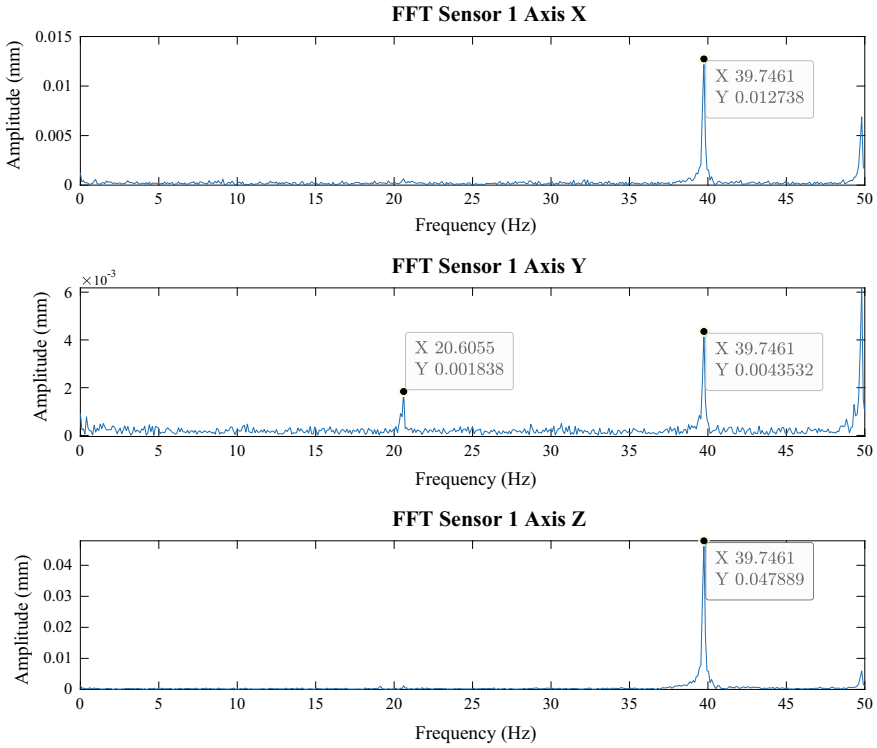

Fig. 4 The vibration mode test sample on sensor 1

Table 4 The natural frequency results (V-B)

Variation	Frequency (Hz)
N	39,746
V1	39,258
V2	39,648
V3	39,063
V4	39,648

The data from the measurement results of the vibration mode in Table 4 shows that the simulated damage affects the natural frequency of the structure. The frequency obtained in N conditions for normal conditions is 39,746 Hz. The V-B damage simulation displays condition frequency V1, V2, V3, and V4, respectively 39,258, 39,648, 39,063, and 39,648 Hz.

Figure 5 shows a graph comparing the amplitude results on each axis recorded on sensor 1. The comparison results show that the amplitude value has increased compared to the N or "normal" condition, with the Z-axis largest deviation. The higher the amplitude was resulting from the vibration, the greater the disturbance/damage to the structure.

The location of the excitation also affects the high amplitude as a source of vibration. The position of V2, which is close to the vibration source, produces the highest vibration amplitude with a value of 0.0722 mm. The position of V4 farthest from the source of the vibration produces the lowest amplitude with a value of 0.0272 mm.

Figure 6 shows a graph comparing the amplitude results on each axis recorded on sensor 2. Based on the observations, the S2 sensor's location, far from the excitation, results in a much smaller amplitude than the S1 sensor. The largest deviation is on the Z-axis, with the highest amplitude occurring in condition V2, namely 0.0390 mm, and the lowest amplitude occurring in condition V4 with a value of 0.0191 mm.

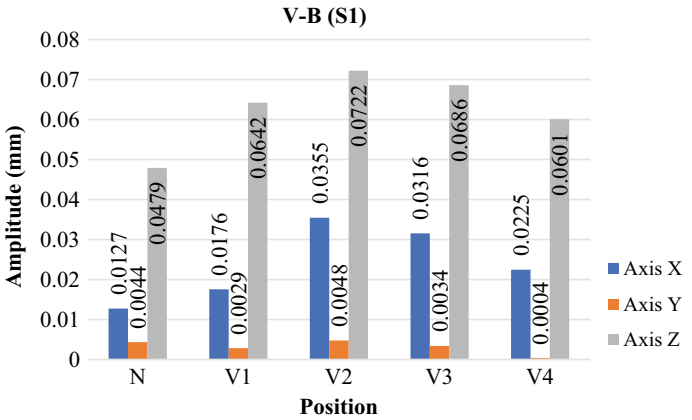

Fig. 5 Comparison of V-B (S1) amplitudes on each axis

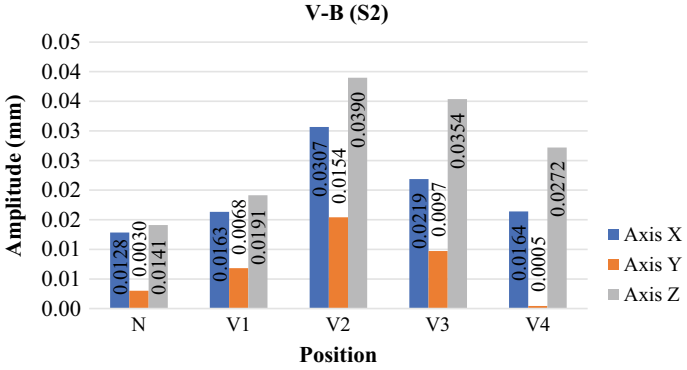

Fig. 6 Comparison of V-B (S2) amplitudes on each axis

4.4 V-50% Vibration Mode Measurement

Table 5 shows the natural frequency of the V-50% damage simulation. The damage simulation V–50% of data collection is at positions on V1, V2, V3, and V4. The natural frequency analyzed by Fast Fourier Transform (FFT) produces natural frequencies in a row from conditions V1, V2, V3, and V4 are 39.648, 39.551, 39.746, and 39.746 Hz.

Figure 7 shows the results of the amplitude comparison of the results of the FFT analysis at S1. The test results show that the dominant amplitude is on the Z-axis for S1. Position V2 provides the highest amplitude with a value of 0.0618 mm for S1. Simultaneously, the lowest value is in the V4 position, with a value of 0.0487 mm. The reason occurs because the position of V2 is close to the source of the vibration. Inversely proportional to the position of the V4, which is far from the source of the vibration.

Figure 8 shows the results of the amplitude comparison of the results of the FFT analysis on S2. The test results on S2 show the same amplitude characteristics as in S1. Position V2 provides the highest amplitude with a value of 0.0219 mm for S1. Simultaneously, the lowest value is in the V4 position, with a value of 0.0138 mm. The reason occurs because the position of V2 is close to the source of the vibration. Inversely proportional to the position of the V4, which is far from the source of the vibration.

Table 5 The natural frequency results (V-50%)

Variation	Frequency (Hz)
V1	39,648
V2	39,551
V3	39,746
V4	39,746

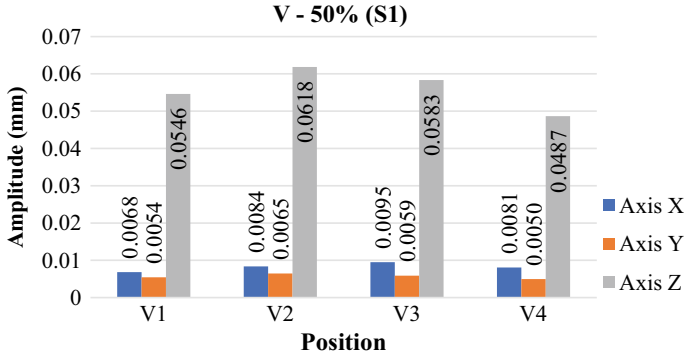

Fig. 7 Comparison of V-50% (S1) amplitudes on each axis

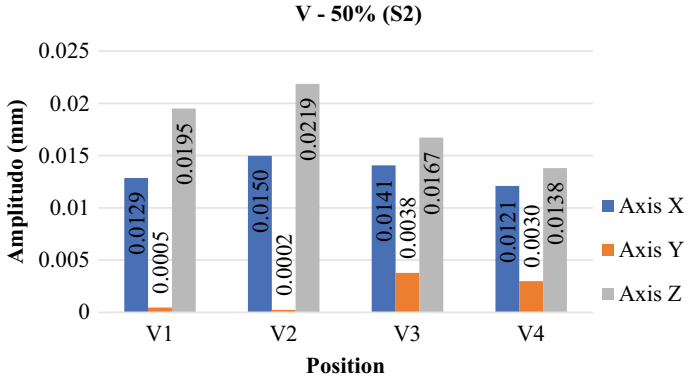

Fig. 8 Comparison of V-50% (S2) amplitudes on each axis

4.5 Comparison of FE Modeling Results versus Bridge Model

Comparing the natural value of the measured frequency due to dynamic load in the FEA model and the experimental model shows relatively good value. The difference resulting from the natural frequency is relatively small, with an error rate of below 10%.

Table 6 compares the natural frequency values in the FE and experimental models. The experimental model shows the highest error rate of 7% at position V2 with a frequency value of 42,191 Hz for the FE model and 39,258 Hz for the experimental model. The lowest error rate is 4% at position V4. This proves that the designed bridge model has a reasonably high similarity in structural characteristics to the FE model simulation.

Table 6 Comparison of frequency results

Position	Frequency (Hz)		Error (%)
	FE	Experimental	
N	41,908	39,746	5
V1	42,191	39,258	7
V2	41,962	39,648	6
V3	41,592	39,063	6
V4	41,232	39,648	4

Table 7 V-B case damping ratio

Position	Sensor 1 (%)	Sensor 2 (%)
V1	0.224	0.229
V2	0.098	0.098
V3	0.145	0.144
V4	0.276	0.283

Table 8 V-50% case damping ratio

Position	Sensor 1 (%)	Sensor 2 (%)
V1	0.096	0.094
V2	0.088	0.087
V3	0.107	0.107
V4	0.282	0.278

4.6 The Damping Ratio of the Great Model

In this damping ratio analysis using the highest amplitude on the Z-axis, then by using Eq. 10, the damping ratio of the structure is obtained, as shown in Tables 7 and 8.

The structural damping ratio analysis on the V-B and V-50% damage simulations above show that the damage simulation performed on the V-B case produces a better damping ratio than the V-50% case. Thus, the damage simulation will affect the damping that occurs in the bridge model due to the decreased structural stiffness.

4.7 Evaluation

In the three-damage simulation model, the bridge model produces varying amplitudes. Figure 9 compares the amplitude results based on three simulations of the damage change in amplitude. The highest amplitude value is used, namely on the Z-axis.

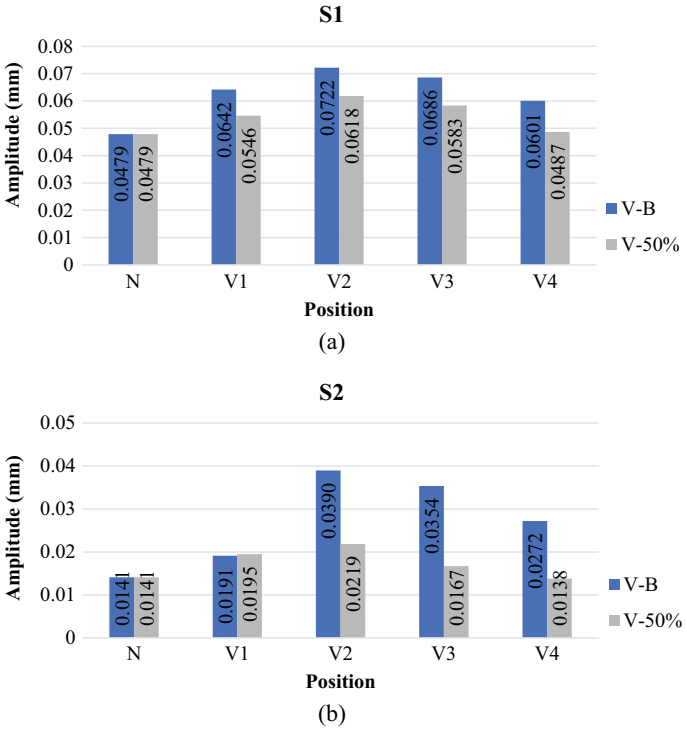

Fig. 9 Comparison of amplitude at V-B and V-50% damage simulation model: **a** sensor 1; **b** sensor 2

Figure 9 shows the comparison of the damage simulation results, namely V-B and V-50% for S1 and S2. The change in amplitude that occurs in the case of V-B damage simulation shows a significant increase. The normal condition (N) comes from the damage simulation V-B, wherein in this condition, the bridge model is in good condition, and then the vibration mode measurements are taken. The level of change in the amplitude of S1 to the damage condition shows that the average increase for the V-P case compared to when the N condition is 38%, and for the V-50% case, it is 17%. For S1, the average increase in the V-B case compared to the N condition was 114%, and for the V-60% case, it was 27%.

Overall, this test succeeded in detecting structural damage locally by looking at amplitude changes based on frequency changes under normal conditions (N) and after damage simulations. When the condition is new or in good condition, the characteristics of the bridge model structure will change characteristics if there is damage to the structure. As a result, the vibration mode generated on the bridge in the form of amplitude tends to increase. Amplitude is a characteristic that shows how much damage has been done. The higher the amplitude obtained, the greater the disturbance/damage that occurs in the structure. The test results [10] show that the differences in natural frequency and amplitude give different responses to vibration mode

and component deformation; this is due to deflection that occurs due to material type, configuration, defects, and others.

5 Conclusion

In this study, the approach taken for monitoring the health of the bridge structure is to use a vibration-based method, which is then carried out by small-scale modeling of the bridge prototype for laboratory testing. The main conclusions of this study are as follows:

1. The natural structure frequency is 39–40 Hz from the vibration test results, with a peak of 39.45 Hz.
2. The natural frequency resulting from normal conditions and four damage positions against the V-B damage simulation in the FE model and the experimental model shows an error rate of below 10%. The most significant error value of 7% in condition V1, and the lowest value of 4% in condition V4.
3. Comparing amplitude measurements in V-P and V-50% shows an increase in amplitude after simulating damage to normal conditions.
4. The characteristics of the bridge model structure when the condition is new or in good condition will change characteristics if there is damage to the structure. As a result, the vibratory mode generated on the bridge in the form of amplitude tends to increase. The amplitude itself is a characteristic that shows how much damage has occurred. The higher the amplitude is showing, the greater the disturbance/damage that occurs in the structure.

The proposed vibration-based SHM approach successfully detects structural damage locally by looking at amplitude changes based on frequency changes under normal conditions (N) and after damage simulation. However, in actual structural conditions, the damage can be caused by various factors such as natural conditions and types of damping. Therefore, this research is still in its early stages. Further, development is needed to model structural damping and change factors in amplitude to identify defects more precisely.

Acknowledgements The author would like to thank the Diponegoro University Structure and Materials Laboratory and the Diponegoro University CNC production process and Laboratory for their assistance in completing this research.

References

1. Mustafa S, Matsumoto Y, Yamaguchi H (2017) Vibration-based health monitoring of an existing truss bridge using energy-based damping evaluation. J Bridg Eng 23(1):04017114. https://doi.org/10.1061/(asce)be.1943-5592.0001159

2. Feng D, Feng MQ (2016) Output-only damage detection using vehicle-induced displacement response and mode shape curvature index. Struct Control Heal Monit 23(8):1088–1107. https://doi.org/10.1002/stc.1829
3. Adi Widyanto S, Widodo Sukamta A, Suprihanto A, Yusuf Tornado F, Nugroho C (2014) Karakteristik peredaman getaran konstruksi model jembatan untuk pengembangan sistem diganosis pola gagal. pp 776–785
4. Ntotsios E, Papadimitriou C, Panetsos P, Karaiskos G, Perros K, Perdikaris PC (2009) Bridge health monitoring system based on vibration measurements. Bull Earthq Eng 7(2):469–483. https://doi.org/10.1007/s10518-008-9067-4
5. Mustafa S, Matsumoto Y (2017) Bayesian model updating and its limitations for detecting local damage of an existing truss bridge. J Bridg Eng 22(7):1–14. https://doi.org/10.1061/(ASCE)BE.1943-5592.0001044
6. Abdo MA-B (2014) In: Structural health monitoring history, applications and future. 1st edn. New York, Open Science
7. Farrar CR, Doebling SW, Nix DA (2001) Vibration-based structural damage identification. Philos Trans R Soc A Math Phys Eng Sci 359(1778):131–149. https://doi.org/10.1098/rsta.2000.0717
8. Pan H, Azimi M, Yan F, Lin Z (2018) Time-frequency-based data-driven structural diagnosis and damage detection for cable-stayed bridges. J Bridg Eng 23(6):1–22. https://doi.org/10.1061/(ASCE)BE.1943-5592.0001199
9. Paz M (1993) In: Dinamika Struktur Teori & Perhitungan, 2nd edn. Jakarta, Erlangga
10. Ofrial MTA, Noerochim L, Hidayat MIP (2017) Analisis Numerikal Frekuensi Natural Pada Poros low pressure boiler feed pump PT.PJB UP Gresik. J Tek ITS 6(1). https://doi.org/10.12962/j23373539.v6i1.21080